ROTATIONAL PROPERTIES OF NEUTRON DRIP-LINE NUCLEI*

W. Nazarewicz,[1–3] J. Dobaczewski,[3,4] M. Matev,[1] S. Mizutori,[4] and W. Satuła[3,4]

[1]Department of Physics and Astronomy, University of Tennessee
Knoxville, Tennessee 37996
[2]Physics Division, Oak Ridge National Laboratory, Oak Ridge, Tennessee 37831
[3]Institute of Theoretical Physics, Warsaw University
ul. Hoża 69, PL-00681 Warsaw, Poland
[4]Joint Institute for Heavy-Ion Research, Oak Ridge National Laboratory
Oak Ridge, Tennessee 37831

(Received May 17, 2001)

We know very little about the structure of neutron-rich, weakly bound nuclei. We know even less about the way they rotate. In this work, the high-spin behavior of deformed neutron-rich nuclei is studied. In particular, quasi-particle Routhian spectra of heavy Er isotopes are discussed within the deformed shell model, and rotational properties and isovector shape deformations of heavy Ne and Mg isotopes are studied with the self-consistent cranked Skyrme-Hartree-Fock theory.

PACS numbers: 21.60.Jz, 21.10.Re, 23.20.-g

1. Introduction

The range of unstable nuclei accessible with Radioactive Nuclear Beam (RNB) facilities opens up enormous opportunities for the study of nuclear structure and exotic new phenomena. Intriguing possibilities occur both at the drip lines and in the long iso-chains of nuclei, especially between the valley of stability and the neutron-rich extreme of nuclear existence.

Exotica in the latter region are almost sure to appear since the mean field in weakly bound neutron-rich nuclei is likely to be modified relative to nuclei near stability, and since reduced nuclear densities and the large reservoir of continuum scattering states should modify residual interactions

---

* Invited talk presented at the *High Spin Physics 2001* NATO Advanced Research Workshop, dedicated to the memory of Zdzisław Szymański, Warsaw, Poland, February 6–10, 2001

among the outermost nucleons [1]. Together, these effects may modify the microscopic foundations of nuclei to the extent that the concept of single-particle motion itself loses validity. Between the regions of known and near-drip-line nuclei lies an extensive zone (typically, 20-40 neutrons wide in medium mass and heavy nuclei) where studies will reveal much about the microscopy of structural evolution and will undoubtedly disclose new types of correlations and collectivity.

RNB experimentation is expected to expand the range of known nuclei. By going to nuclei with extreme N/Z ratios, one can magnify the isospin-dependent terms of the effective interaction (which are small in "normal" nuclei). On the other hand, by going to very high spins, one can probe those components of the effective interaction which depend on the spin degrees of freedom. Clearly, by studying *the response of neutron-rich nuclei to rotation*, one can obtain very unique information about basic properties of the nuclear many-body system.

This paper contains discussion of high-spin phenomena that are expected to occur in neutron-rich nuclei. Most of the examples shown are very "theoretical". The authors are well aware that many nuclei discussed in this study cannot be accessed experimentally. Nevertheless, the "impossible-to-reach" nuclei, such as ^{208}Er, represent extreme cases where certain structual effects manifest themselves in a clear and transparent way. Fingerprints of these effects will be looked for experimentally by systematically extending our knowledge of the neutron-rich *terra incognita.*

2. Spectroscopy of Neutron-Rich Nuclei: the Current Status

High spin spectroscopy in neutron-rich nuclei represents a formidable experimental challenge. The fusion evaporation reactions which are commonly used to populate high-spin states give rise to evaporation residua which are proton-rich. Therefore, even stable nuclei are not accessible using the standard in-beam techniques. Consequently, a number of methods have been applied to obtain spectroscopic information on neutron-rich systems [2, 3].

One way of carrying out spectroscopic studies in the neutron-rich systems is to analyze the prompt gamma rays from nascent fission fragments (produced either in spontaneous fission or in heavy-ion-induced fission). In such measurements it is possible to approach spectroscopically relatively neutron-rich nuclei [4, 5, 6, 7, 8, 9, 10]. Rotational structures in neutron-rich nuclei have also been studied using transfer reactions [11, 12], incomplete fusion [13], neutron-induced fission [14, 15], and deep inelastic reactions [16, 17]. The technique of Coulomb excitation at intermediate energies (employing in-flight isotopic separation of projectile fission fragments) has been used to study the lowest excited states in very neutron-rich light and medium-mass nuclei [3, 18, 19, 20]. Very recently, it was possible, for the first time, to perform spectroscopic measurements with accelerated radioactive neutron-rich beams using coulex and fusion-evaporation reactions [21]. This new development offers a number of exciting opportunities for nuclear structure studies on the neutron-rich side.

However, in spite of many experimental efforts, detailed information on high-spin properties of neutron-rich nuclei still remains scarce. This is most unfortunate, since - in many cases - even by adding as few as 2-3 neutrons to the last known isotope, one enters a region where new phenomena occur. A classic example is the region of the neutron-rich Ba-Ce nuclei which exhibit strong octupole correlations, and even octupole deformations, manifesting themselves in the presence of alternating-parity bands [22]. These nuclei are spontaneous fission products; hence some spectroscopic information, mainly at medium spins, already exists. One of the most interesting regions on the neutron-rich side of the stability valley are the nuclei around ^{102}Zr, also produced in spontaneous fission, where a variety of deformation effects and shape changes due to quasi-particle alignment are expected as a function of angular momentum [23]. From the theoretical point of view, probably the most attractive nuclei in this mass region are the systems near ^{104}Mo and ^{108}Ru, which are predicted to have stable collective triaxial shapes ($\gamma\approx-30^{\circ}$). Although the question of whether they are γ-soft or γ-deformed at low spins has not yet been settled, these nuclei seem to be ideal for testing theoretical models of nuclear triaxiality. In particular, at higher spins, where the triaxial minima are predicted to be deeper, the shape with $\gamma\approx-30^{\circ}$ can give rise to interesting selection rules associated with the effective C_4 symmetry of the Hamiltonian [24]. The presence of static triaxial deformations is prerequisite for the existence of chiral bands[25] and wobbling bands[26] - new collective modes of the rotating nucleus. Figure 1 shows the total Routhian surfaces for ^{108}Ru calculated within the cranked shell correction approach with the Woods-Saxon average potential and monopole pairing. This heavy ruthenium isotope is triaxial in its ground state, and the corresponding collective triaxial minimum with $\beta_2\approx0.28$ and $\gamma\approx-30^{\circ}$ is yrast in a wide range of rotational frequencies. The alignment of $h_{11/2}$ neutrons, $g_{9/2}$ protons, followed by the second $h_{11/2}$ neutron alignment, produces triaxial shapes with $\beta_2\approx0.2$, $\gamma\approx-45^{\circ}$. (For recent experimental data on high-spin behavior of ^{108}Ru, see Ref. [8].) At high spins, transition to superdeformed shapes is predicted. According to calculations [23], the most favorable candidates for superdeformation in this mass region are ^{100}Mo and $^{108-112}$Ru.

It is only in light nuclei that it has been possible to approach the neutron drip line experimentally and to obtain some spectroscopic information on nuclei with an extreme neutron excess. The neutron-rich nuclei with $N\approx20$

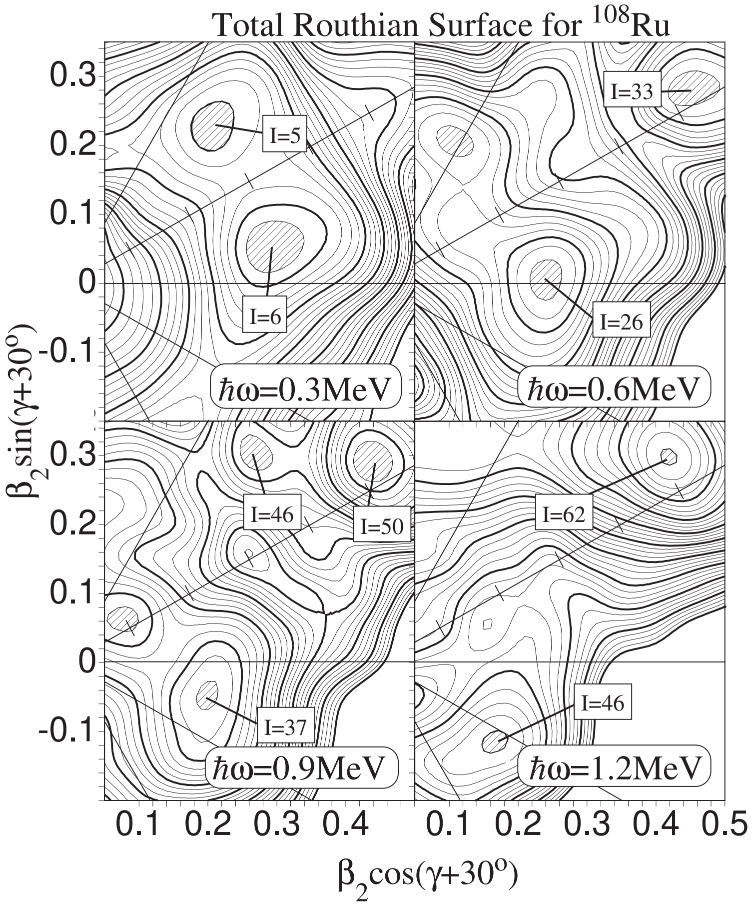

Fig. 1. Total Routhian surfaces in the (β_2, γ)-plane for the (π=+, r=1) quasiparticle vacuum configuration of ^{108}Ru at four values of rotational frequency: $\hbar\omega$=0.3, 0.6, 0.9, and 1.2 MeV. At each (β_2, γ) point the total Routhian has been minimized with respect to hexadecapole deformation β_4. The distance between thick contour lines is 1 MeV, while between the thin contour line it is 250 keV. The angular momentum values at local minima are indicated. (From Ref. [23].)

are spectacular examples of coexistence between spherical and deformed configurations in the sd shell ($8 \leq Z, N \leq 20$). A classic example is the "semi-magic" nucleus $^{32}_{12}$Mg$_{20}$, which has a very low-lying 2^+ state at 886 keV [27] and an anomalously high value of the two-neutron separation energy S_{2n}. Deformed shapes in this mass region have been inferred from the intermediate-energy Coulomb excitation studies [28, 19, 20] which provided information on position and collectivity of the lowest 2^+ and 4^+ states in

^{32,34}Mg. Many calculations based on the mean-field theory have predicted deformed ground states in nuclei from the ^{32}Mg region (sometimes dubbed as an "island of inversion"). The origin of the shape coexistence effects around ^{32}Mg can be traced back to the crossing between the prolate-driving [330]1/2 *intruder level*, originating from the $1f_{7/2}$ shell, and the oblate-driving [201]3/2 *extruder level*; see Fig. 2 and Ref. [30] for more discussion. Another, recently discovered, island of inversion are the neutron-rich nuclei from the pf shell centered around $^{44}_{16}S_{28}$ [31, 18, 32]. According to the mean-field calculations [30, 33, 34], deformation effects around ^{44}S can be attributed to the appreciable breaking of the N=28 core. In the shell-model language, islands of inversion have their roots in the monopole effect caused by the proton-neutron residual interaction [35, 36].

3. Special Features of Neutron-Rich Nuclei

There are many theoretical arguments suggesting that the nuclei near the neutron drip line represent another form of nuclear life. For instance, some calculations predict [1, 37, 38, 39] that the shell structure of neutron drip-line nuclei is different from what is known around the beta-stability valley. According to other calculations [40], a reduction of the spin-orbit splitting in neutron-rich nuclei is expected. An interesting question to ask in the context of "islands of inversion" discussed in Sec. 2 is to what extent the "traditional" explanation in terms of intruder states, proton-neutron-correlations, pairing, etc., needs to be modified in the neutron-rich nuclei, where the quenching of the known magic gaps is expected. Clearly, the reduction of the N=20 and 28 gaps far from stability can lower the excitation energy of the deformed intruder configuration; hence it can enhance the shape transition. However, before one addresses this question in a systematic way by properly taking into account competition between mean field and pairing, one should avoid calling the shape transition around ^{32}Mg and ^{44}S as evidence for the shell gap quenching.

Halo nuclei are the best known examples of possible exotica. They are examples of physics on the threshold of nuclear binding. The predicted phenomena of low-density neutron skins is another, which is topologically similar to a halo, but quite different in microscopic origin [41]. Correlations due to pairing, core polarization, and clustering are crucial in weakly bound nuclei. In a drip-line system, the pairing interaction and the presence of skin excitations (soft modes) could invalidate the picture of a nucleon moving in a single-particle orbit [39, 42, 43, 44, 45]. According to theory, the low-ℓ spectroscopic strength is dramatically broadened when approaching the neutron drip line. Also, in the presence of large neutron excess, strong isovector effects are expected. For instance, some calculations predict nuclear con-

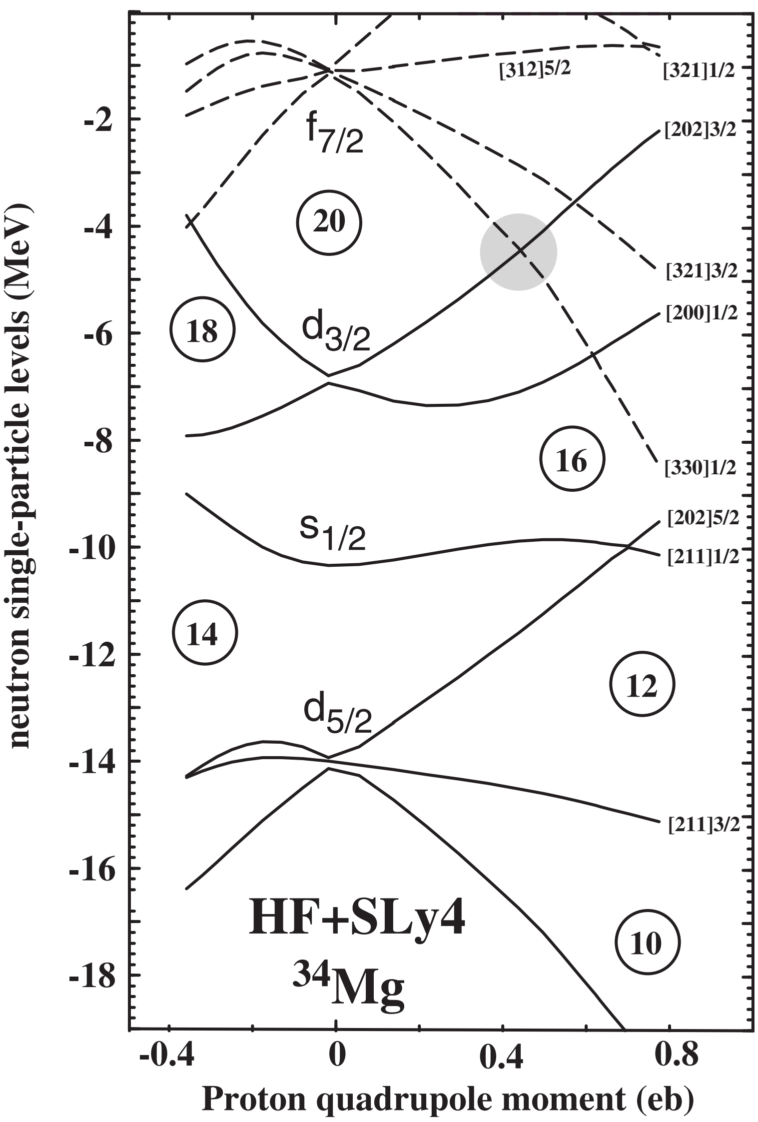

Fig. 2. Single-neutron levels in ^{34}Mg as a function of the proton charge quadrupole moment Q_{20} (Q_{22}=0) calculated in the HF+SLy4 model. The crossing between the [330]1/2 intruder level and the [201]3/2 extruder level is indicated. (From Ref. [29].)

figurations having different proton and neutron deformations [33, 34, 46]. However, in order to address this particular question properly, pairing correlations need to be properly taken into account. In the following, we carry out simplified calculations which focus on some of the physics aspects mentioned above.

4. Quasi-Particle Excitations in Rotating Neutron-Rich Nuclei

Nuclear high-spin behavior is always strongly impacted by the single-particle shell structure. The order of single-particle states around the Fermi level determines the deformability of the nucleus, its moment of inertia, and the Coriolis coupling. Consequently, any changes to the shell structure are going to show up at high spins. In this section, we discuss several signatures of shell quenching as seen through the quasi-particle spectra of rotating nuclei.

The major consequence of the modified shell structure in neutron-rich nuclei is the change in the placement of unique-parity orbitals which revert to their original shells. Since high-j states are the building blocks of nuclear rotation (they are influenced most by the Coriolis coupling), this shift is expected to impact a number of observables. In order to illustrate the effect of shell quenching on nuclear rotation, we performed the deformed shell-model analysis of quasi-neutron spectra in extremely neutron-rich deformed nuclei. According to recent Skyrme-HFB calculations [47], the largest deformations in heavy neutron drip-line nuclei are expected in three regions: around ^{100}Zn, ^{146}Pd, and in the Rare Earths (Gd, Dy, Er, and Yb). It is to be noted that the microscopic-macroscopic finite range droplet model [48] also predicts deformations in these regions.

Figure 3 displays the energy difference between the spherical $j_{15/2}$ level and the centers of gravity, $e_{sh}(\mathcal{N})$, of the normal-parity $\mathcal{N}$=6 and $\mathcal{N}$=7 shells as a function of a. At the standard value of a=0.7 fm, the $j_{15/2}$ level lies close to the center of the $\mathcal{N}$=6 shell, and almost 1 $\hbar\omega_0$ below the $\mathcal{N}$=7 shell. With increasing a, the intruder shell gradually moves towards the $\mathcal{N}$=7 shell. We checked that the inclusion of deformation does not change this pattern.

The calculations were performed with the cranked Woods-Saxon (WS) model with the constant pairing gap approximation [49, 50]. In order to mock up the self-consistent spectra, the WS neutron diffuseness parameter a has been varied in order to reproduce the behavior of spherical single-neutron levels obtained in HFB. For the details of the calculations, we refer the reader to Ref. [51].

The effect of the large diffuseness on the rotational properties of high-j states is rather weak. Figure 4 (top) displays the decoupling parameters of the [770]1/2 and [660]1/2 Nilsson levels as a functions of a. Although the decoupling parameters do decrease with the diffuseness, for the realistic

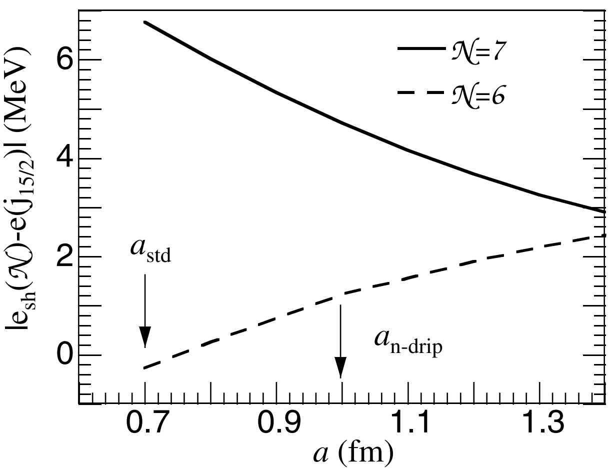

Fig. 3. Energy difference between the spherical $j_{15/2}$ level and the centers of gravity of the $\mathcal{N}=6$ and $\mathcal{N}$=7 shells as a function of the neutron diffuseness parameter a in the spherical WS potential. Calculations were performed for ^{208}Er.

values of a, they are still fairly close to the pure single-j limits of $j+1/2$ indicated by arrows in Fig. 4. As is seen in Fig. 4 (bottom), the effect on the quasi-particle alignment is even weaker.

It is the pattern of quasi-particle excitations where more deviations from the standard situation are expected. Consider, e.g., two N=140 isotones: ^{230}Th and the very neutron-rich nucleus ^{208}Er. In the case of ^{230}Th, the neutron Fermi level lies between the Ω=5/2 and Ω=7/2 members of the $j_{15/2}$ shell. In ^{208}Er, due to increased diffuseness, the intruder shell moves up (cf. Fig. 3) and the neutron Fermi level lies at the bottom of the shell, i.e., in the vicinity of the [770]1/2 Nilsson level. As seen in Fig. 5, this changes the signature splitting of the lowest negative parity states and also the position of the higher-frequency neutron crossings. A similar situation is expected around ^{146}Pd, where the $i_{13/2}$ intruder is shifted up in energy.

5. Rotation of Neutron-Rich Ne and Mg Isotopes

To obtain a quantitative understanding of measured quadrupole moments, we performed systematic cranking calculations without pairing using the self-consistent cranked Skyrme Hartree-Fock (HF) method (code HFODD [52, 53]) with the Skyrme parametrization SLy4 [54, 55]. This method has shown to provide an accurate description of various properties of rotational bands in different mass regions (see, e.g., Refs. [56, 57, 58]). For the details pertaining to theoretical calculations, see forthcoming Ref. [29].

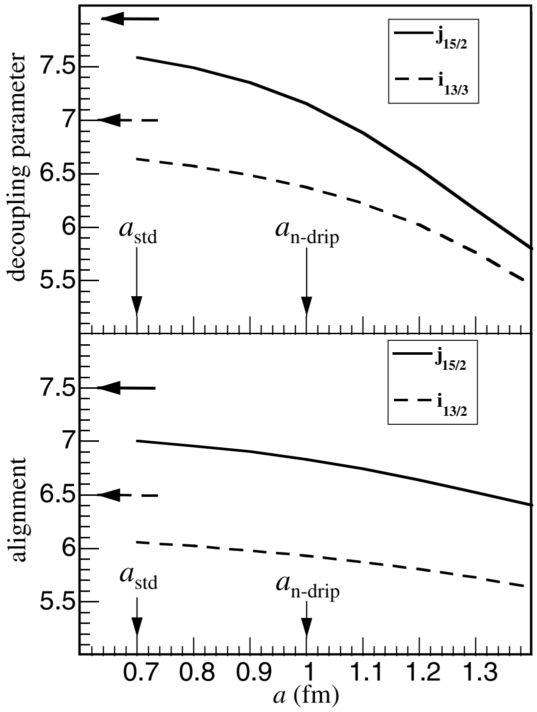

Fig. 4. Decoupling parameters of the [770]1/2 and [660]1/2 levels (top) and the quasi-particle alignments of the lowest $\mathcal{N}=6$ and $\mathcal{N}$=7 quasi-particle Routhians (at $\hbar\omega$=0.1 MeV, bottom) as functions of the neutron diffuseness of parameter. Calculations were performed at β_2=0.25 and Δ=1 MeV.

Here we only mention that the intrinsic configurations are labeled by means of total occupation numbers in each parity-signature sector $N_{\pi,r}$: $[N_{+,-i}$, $N_{+,+i}$, $N_{-,-i}$, $N_{+,+i}]$. For instance, the ground-state configuration of ^{30}Ne (two protons in the $d_{5/2}$ orbital; the neutron sd shell completely filled) can be written as $[2233]_p[7733]_n$. As seen in Fig. 2, the deformed intruder configurations in ^{30}Ne and ^{32}Mg can be associated with 2-particle, 2-hole neutron excitation to the $f_{7/2}$ shell; hence it can be written as $[6644]_n$. The corresponding neutron single-particle Routhian diagram for ^{30}Ne is shown in Fig. 6.

Calculations of rotational bands were carried out for the deformed configurations in ^{30,32,34,36,38}Ne and ^{32,34,36,38,40}Mg. Since pairing correlations were ignored, we consider these calculations as exploratory. Here, our main objective is to investigate the effect of fast rotation on properties of weakly bound systems with a very large neutron excess. For the deformed bands

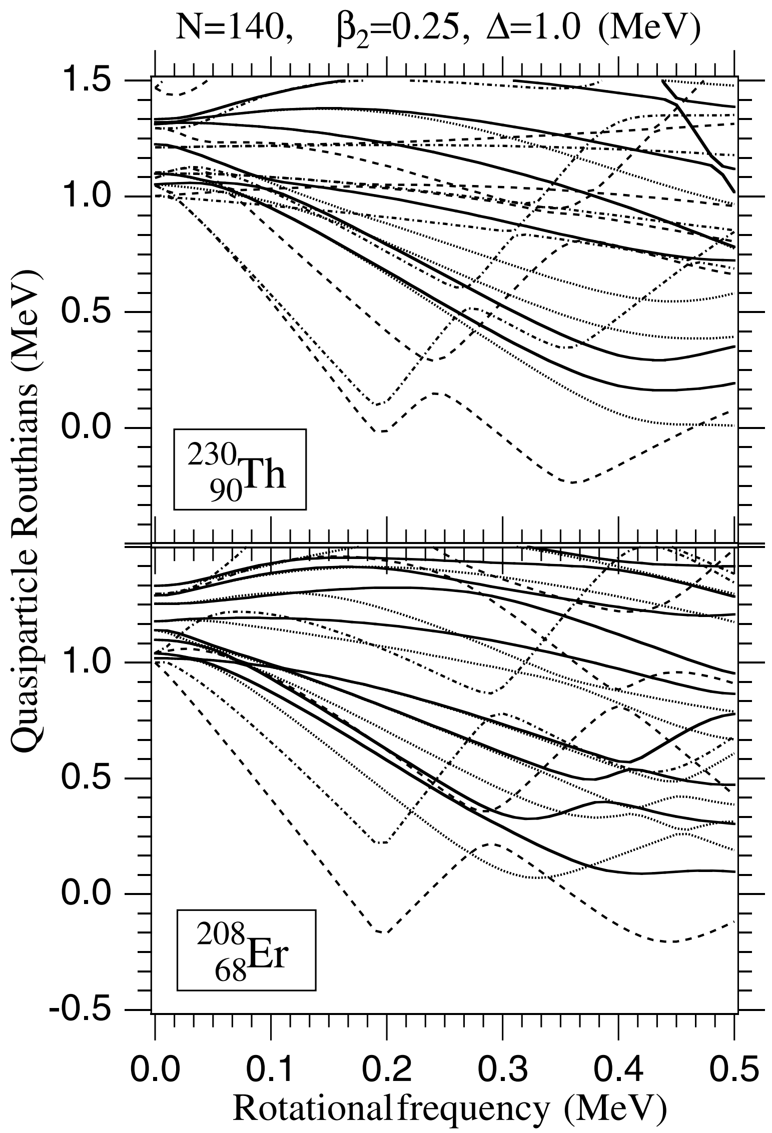

Fig. 5. Quasi-particle neutron diagram calculated in the WS model for two N=140 isotones: ^{230}Th and ^{208}Er. Calculations were performed at β_2=0.25 and Δ=1 MeV.

considered, the proton configurations for Ne and Mg are always $[2233]_p$ and $[3333]_p$, respectively. (There are no crossings between positive and negative-parity Routhians for Z=10 and 12 in the range of angular momentum discussed.) As far as the neutrons configurations are concerned, we assumed

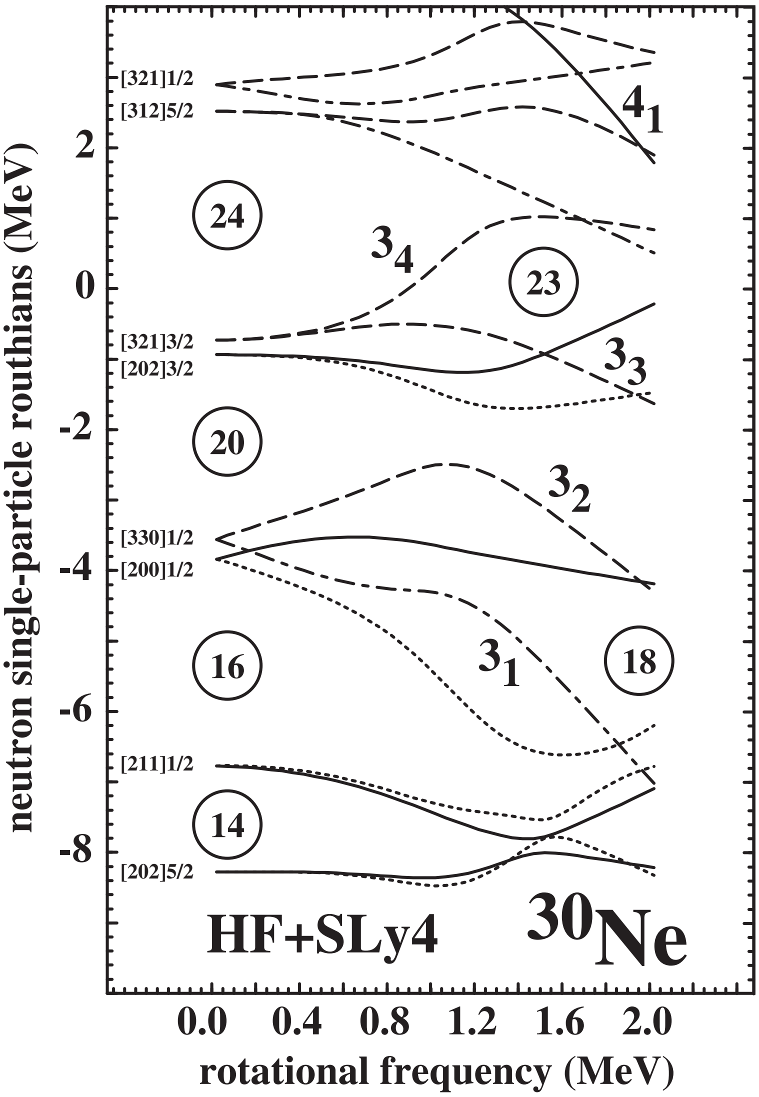

Fig. 6. Neutron single-particle Routhians in ^{30}Ne calculated in the HF+SLy4 model for the $[2233]_p$ $[6644]_n$ intruder configuration.

$[6644]_n$ for N=20, $[6655]_n$ and $[7744]_n$ for N=22, $[7755]_n$ for N=24, $[7766]_n$ for N=26, and $[7777]_n$ for N=28. These configurations correspond to the lowest deformed bands in the neutron-rich Ne and Mg nuclei investigated.

From the calculated components of the quadrupole moment, Q_{20} and Q_{22}, one can extract the Bohr quadrupole deformation parameters β_2 and

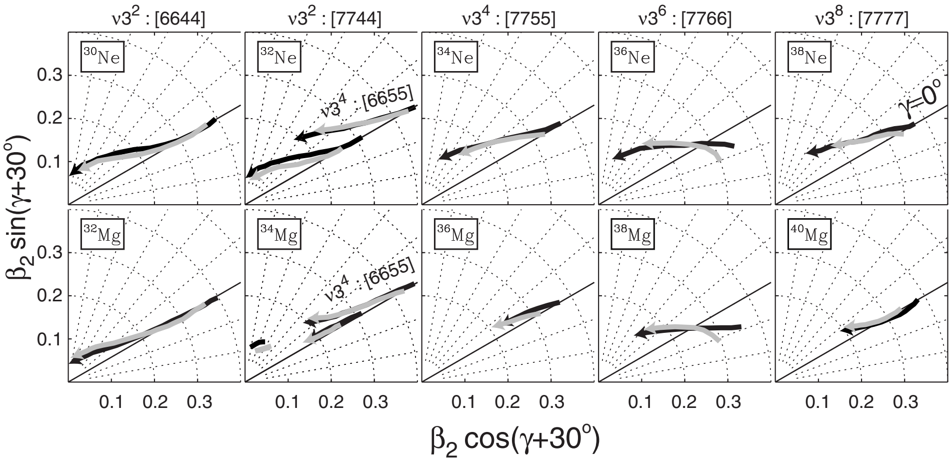

Fig. 7. Neutron (gray arrows) and proton (black arrows) quadrupole deformations β_2 and γ as functions of rotational frequency for the deformed bands in ^{30,32,34,36,38}Ne and ^{32,34,36,38,40}Mg.

γ [53]:

$$\tan\gamma = \frac{Q_{22}}{Q_{20}}, \quad \beta_2 = \sqrt{\frac{\pi}{5}}\frac{\sqrt{Q_{20}^2 + Q_{22}^2}}{N_\tau\langle r^2\rangle}, \tag{1}$$

where τ=1 (–1) for neutrons (protons), and N_1=N and N_{-1}=Z. Figure 7 shows the calculated proton and neutron deformation trajectories in the (β_2, γ) plane as functions of rotational frequency. In general, the differences between proton and neutron deformations are rather small. They are most pronounced at low spins; the proton and neutron shapes become similar at angular momenta close to the termination limit. The strongest isovector effects are predicted in the N=26 isotones where $\Delta\beta_2 \equiv \beta_2^p - \beta_2^n$ reaches 0.05 at low spins. It is interesting to see that for ^{36}Ne $\Delta\beta_2$ changes sign from postive ($\beta_2^p > \beta_2^n$) at low spins to negative ($\beta_2^p < \beta_2^n$) at very high angular momenta. The pattern represented in Fig. 7 is characteristic of rotational structures built upon relatively few valence nucleons. The loss of collectivity is rather fast due to the alignment of $f_{7/2}$ neutrons, which leads to the band termination at relatively low spins (e.g., I=12 for ^{30}Ne).

An interesting question which is often asked in the context of rotational motion of weakly bound neutron-rich nuclei is whether the weakly bound neutrons could be kicked off the nucleus due to the large centrifugal force. To shed some light on this problem, Fig. 8 displays the predicted rms proton and neutron radii as functions of ω. Generally, rms radii very weakly depend

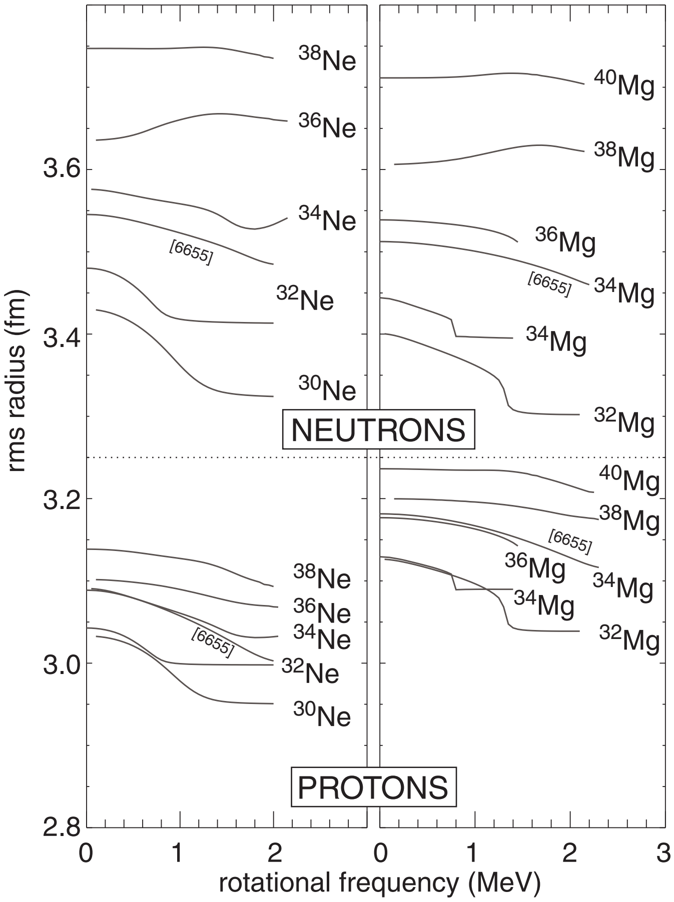

Fig. 8. Neutron and proton rms radii as a function of rotational frequency for the deformed bands in ^{30,32,34,36,38}Ne and ^{32,34,36,38,40}Mg.

on rotation. The small reduction calculated in some cases comes primarily from the decrease in β_2 along the band termination path. However, the deformation effect is weaker compared to the bulk dependence of radii on Z and N.

Considering the results presented in Figs. 7 and 8, one can conclude that the isovestor effects are not very pronounced at high angular momenta in the neutron-rich Ne and Mg isotopes. This is not entirely unexpected. In these nuclei, the valence neutrons occupy $f_{7/2}$ high-j intruder states which, due to their large orbital angular momentum (i.e., large centrifugal barrier), are fairly well localized within the nuclear volume in spite of their weak binding. One can say that in most cases, as a result of the Coriolis force, the low-ℓ states (which are natural candidates for halo effects) are going to be crossed at high rotational frequencies by the high-ℓ intruder orbitals. Consequently, the tendency to develop a halo should be reduced at high spins. The full analysis of our calculations of the Ne and Mg isotopes, containing the discussion of the moments of inertia, will be presented in a forthcoming paper [29]. The general conclusion is that the response of very neutron-rich nuclei to rotation is fairly "normal"; no decoupling of the valence (skin) neutrons at high spins is predicted.

6. Conclusions

The main objective of this brief review was to discuss various facets of high-spin physics on the neutron-rich side of the stability valley. The vast unexplored territory of very neutron-rich nuclei offers prospects for new physics. The combination of the large neutron excess and weak binding are believed to create particle-hole and pairing fields which are rather different from those in nearly stable nuclei. In spite of many experimental difficulties, spectroscopic information, mainly on light nuclei and low-spin states, is arriving steadily.

What is the response of the neutron drip-line nuclei, the large, diffused, and possibly superfluid many-body systems to rotation? Both the schematic and self-consistent calculations contained in this paper give interesting insights to this question. On the one hand, the variation of the neutron shell structure with neutron number, mainly influencing the position of the high-j unique-parity shell, is expected to modify the pattern of quasiparticle excitations in the rotating nucleus. On the other hand, since the Coriolis force mainly acts on the high-j orbitals which are strongly localized within the nuclear volume because of the large centrifugal barrier, no strong isovector effects (due to neutron halo or skin) are expected at high spins. For instance, our unpaired calculations indicate that proton and neutron deformations are very similar at high rotational frequencies. The fascinating question, which still remains to be answered, is what is the interplay between rotation, pairing, and extreme isospin. The recent impressive progress in theoretical modeling of high-spin nuclear states, as presented and discussed during this conference, makes us optimistic that this question will soon be answered.

An experimental excursion into uncharted territories of the chart of the nuclides, promised by the new-generation RNB facilities, gamma-ray tracking arrays, and mass/charge separators, will offer many excellent opportunities for nuclear structure research. What is most exciting, however, is that there are many unique features of neutron-rich nuclei that give prospects for entirely new phenomena likely to be different from anything we have observed to date.

This work was supported in part by the U.S. Department of Energy under Contract Nos. DE-FG02-96ER40963 (University of Tennessee), DE-FG05-87ER40361 (Joint Institute for Heavy Ion Research), DE-AC05-00OR 22725 with UT-Battelle, LLC (Oak Ridge National Laboratory), and by the Polish Committee for Scientific Research (KBN).

REFERENCES

[1] J. Dobaczewski and W. Nazarewicz, Phil. Trans. R. Soc. Lond. A **356**, 2007 (1998).

[2] J.L. Durell, AIP Conference Proceedings **495**, 179 (1999).

[3] T. Glasmacher, Ann. Rev. Nucl. Part. Sci. **48**, 1 (1998).

[4] W. Gelletly *et al.*, in *Nuclear Structure of the Zirconium Region*, ed. by J. Eberth, R.A. Meyer, and K. Sistemich, (Springer-Verlag, 1988), p. 102.

[5] M.A.C. Hotchkis *et al.*, Phys. Rev. Lett. **64** (1990) 3123.

[6] M.A.C. Hotchkis *et al.*, Nucl. Phys. **A530** (1991) 111.

[7] Q.H. Lu *et al.*, Phys. Rev. **C52**, 1348 (1995).

[8] I. Deloncle *et al.*, Eur. Phys. J. A **8**, 177 (2000).

[9] A. Korgul *et al.*, Eur. Phys. J. A **7**, 167 (2000).

[10] X.Q. Zhang *et al.*, Phys. Rev. **C61**, 014305 (2000).

[11] R. Estep *et al.*, Phys. Rev. **C39**, 76 (1989).

[12] C.Y. Wu *et al.*, Phys. Rev. **C57**, 3466 (1998).

[13] H. Dejbakhsh and S. Bouttchenko, Phys. Rev. **C52**, 1810 (1995).

[14] J.A. Shannon *et al.*, Phys. Lett. **336B**, 136 (1994).

[15] S. Schoedder, G. Lhersonneau, A. Wohr, G. Skarnemark, J. Alstad, A. Nahler, K. Eberhardt, J. Aysto, N. Trautmann, and K.-L.Kratz, Z. Phys. **A352**, 237 (1995).

[16] S.J. Asztalos *et al.*, Phys. Rev. **C60**, 044307 (1999).

[17] G.J. Lane *et al.*, Nucl. Phys. A682, 71c (2001).

[18] T. Glasmacher *et al.*, Phys. Lett. B **395**, 163 (1997).

[19] M. Belleguic *et al.*, Nucl. Phys. **A682**, 136c (2001).

[20] K. Yoneda *et al.*, Phys. Lett. **499B**, 233 (2001).

[21] D.C. Radford *et al.*, to be published; HRIBF News **8**, No. 4, http://www.phy.ornl.gov/hribf/usersgroup/news/.

[22] P. Butler and W. Nazarewicz, Rev. Mod. Phys. **68**, 349 (1996).

[23] J. Skalski, S. Mizutori, and W. Nazarewicz, Nucl. Phys. **A617**, 282 (1997).

[24] I. Hamamoto, Phys. Lett. B **193**, 399 (1987).

[25] S. Frauendorf, in these proceedings

[26] I. Hamamoto *et al.*, in these proceedings

[27] C. Détraz *et al.*, Phys. Rev. **C19**, 164 (1979).

[28] T. Motobayashi *et al.*, Phys. Lett. B **346**, 9 (1995).

[29] M. Matev *et al.*, to be published 2001.

[30] P.-G. Reinhard, D.J. Dean, W. Nazarewicz, J. Dobaczewski, J.A. Maruhn, and M.R. Strayer, Phys. Rev. **C60**, 014316 (1999).

[31] H. Scheit *et al.*, Phys. Rev. Lett. **77**, 3967 (1996).

[32] F. Azaiez, Acta Phys. Hung. N.S. **12**, 241 (2000).

[33] T.R. Werner, J.A. Sheikh, W. Nazarewicz, M.R. Strayer, A.S. Umar, and M. Misu, Phys. Lett. **B333**, 303 (1994).

[34] T.R. Werner, J.A. Sheikh, M. Misu, W. Nazarewicz, J. Rikovska, K. Heeger, A.S. Umar, and M.R. Strayer, Nucl. Phys. **A597**, 327 (1996).

[35] K. Heyde and J.L. Wood, J. Phys. **G17**, 135 (1991).

[36] J.L. Wood, K. Heyde, W. Nazarewicz, M. Huyse, and P. van Duppen, Phys. Rep. **215**, 101 (1992).

[37] F. Tondeur, Z. Phys. **A288**, 97 (1978).

[38] J. Dobaczewski, I. Hamamoto, W. Nazarewicz, and J.A. Sheikh, Phys. Rev. Lett. **72**, 981 (1994).

[39] J. Dobaczewski, W. Nazarewicz, T.R. Werner, J.-F. Berger, C.R. Chinn, and J. Dechargé, Phys. Rev. **C53**, 2809 (1996).

[40] G.A. Lalazissis, D. Vretanar, W. Poschl, and P. Ring, Phys. Lett. **418B**, 7 (1998).

[41] S. Mizutori, J. Dobaczewski, G. A. Lalazissis, W. Nazarewicz, and P.-G. Reinhard, Phys. Rev. C **61**, 044326 (2000).

[42] W. Pöschl, D. Vretenar, G.A. Lalazissis, and P. Ring, Phys. Rev. Lett. **79**, 3841 (1997).

[43] K. Bennaceur, J. Dobaczewski, and M. Płoszajczak, Phys. Rev. **C60**, 034308 (1999).

[44] K. Bennaceur, J. Dobaczewski, and M. Płoszajczak, Phys. Lett. **B496**, 154 (2000).

[45] S.A. Fayans, S.V. Tolokonnikov, and D. Zawischa, Phys. Lett. **491B**, 245 (2000).

[46] T. Misu, W. Nazarewicz, and S. Åberg, Nucl. Phys. **A614**, 44 (1997).

[47] J. Dobaczewski, M. Stoitsov, and W. Nazarewicz, to be published.

[48] P. Möller, J.R. Nix, W.D. Myers, and W.J. Swiatecki, Atom. Data and Nucl. Data Tables **59**, 185 (1995).

[49] S. Ćwiok, J. Dudek, W. Nazarewicz, J. Skalski, and T. Werner, Comput. Phys. Commun. **46**, 379 (1987).

[50] W. Nazarewicz, J. Dudek, R. Bengtsson, T. Bengtsson, and I. Ragnarsson, Nucl. Phys. **A435** (1985) 397.

[51] S. Mizutori *et al.*, to be published 2001.

[52] J. Dobaczewski and J. Dudek, Comput. Phys. Commun. **102**, 166 (1997); **102**, 183 (1997)

[53] J. Dobaczewski and J. Dudek, Comput. Phys. Commun. **131**, 164 (2000).

[54] E. Chabanat, P. Bonche, P. Haensel, J. Meyer, and F. Schaeffer, Physica Scripta **T56**, 231 (1995).

[55] E. Chabanat, *Interactions effectives pour des conditions extrêmes d'isospin*, Université Claude Bernard Lyon-1, Thesis 1995, LYCEN T 9501, unpublished.

[56] W. Satuła, J. Dobaczewski, J. Dudek, and W.Nazarewicz, Phys. Rev. Lett. **77**, 5182 (1996).

[57] N. El Aouad *et al.*, Nucl. Phys. A **676**, 155 (2000).

[58] M.A. Riley *et al.*, in these proceedings.